DETECTING AMAZONIAN DEFORESTATION USING MULTITEMPORAL THEMATIC MAPPER IMAGERIES AND SPECTRAL MIXTURE ANALYSIS

Dengsheng Lu, Assistant Research Scientist
Center for the Study of Institutions
Population, and Environmental Change (CIPEC)
Indiana University
Bloomington, Indiana
dlu@indiana.edu

Mateus Batistella, Research Manager
Brazilian Agricultural Research Corporation
EMBRAPA Satellite Monitoring
Campinas, São Paulo, Brazil
mb@cnpm.embrapa.br

Emilio Moran, James H. Rudy Professor, Director of ACT and Co-Director of CIPEC
Anthropological Center for Training and Research on Global Environmental Change (ACT)
Indiana University
Bloomington, Indiana
moran@indiana.edu

ABSTRACT

Linear spectral mixture analysis (LSMA) and multitemporal Thematic Mapper (TM) data were used to detect deforestation in Altamira and Machadinho, Brazilian Amazon. Standardized principal component analysis was used to transform TM data into uncorrelated principal components (PCs). Three endmembers were selected and an unconstrained least root-mean squared error solution was used to unmix the first four PCs into three fraction images. Mature forest classification was implemented using thresholds and deforestation detection using binary image overlay. This study indicates that LSMA is an effective method to identify mature forest and detect deforested areas with high accuracies.

INTRODUCTION

The Brazilian Amazon contains the largest continuous tropical rain forest in the world, representing a potentially large source of carbon/greenhouse gas emissions (Fearnside, 1998). In the Amazon basin the deforestation rates rose sharply during the 1970s and 1980s and more recently during the mid-1990s due to road building, colonization projects, logging, and agropastoral expansion associated with national political and economic policies (Moran et al., 1994; Skole et al., 1994; Alves, 2002). The estimated deforestation rate was 15,000–20,000 km^2 per year between 1978 and 1988 (Skole et al., 1994), approximately 17,000 km^2 per year between 1988 and 1996 (INPE, 1998), and approximately 18,000 km^2 in 2000 (INPE, 2002). Previous research has shown that the loss of Amazonian forests corresponded to about 7% of the total carbon dioxide (CO_2) emissions provoked by fossil fuel emission (Moran et al., 1994). Deforestation typically leads to tremendous effects on climate change, biological diversity, the hydrologic cycle, and soil erosion and degradation (Shukla et al., 1990; Houghton, 1991; Skole and Tucker, 1993). Therefore, accurately detecting deforestation area and rate has become an urgent task.

Although many change detection methods have been developed (Singh, 1989; Mouat et al., 1993; Deer, 1995; Coppin and Bauer, 1996; Jensen, 1996; Jensen et al., 1997; Yuan et al., 1998; Serpico and Bruzzone, 1999), most of them can only provide change and non-change information but cannot accurately provide specific change information such as deforestation. Because of the important effects of mature forest deforestation on climate and ecosystems, accurate deforestation detection is valuable to better understand the relationships between deforestation and the components of atmosphere and ecosystem change. Thus, an effective method to digitally detect deforestation areas and rates is needed. Some previous research has indicated that linear spectral mixture analysis (LSMA) is a promising tool in land-cover classification and change detection for tropical regions (Adams et al., 1995; Roberts et

al., 1998; Lu et al., in press). This paper focuses on the detection of deforested areas and deforestation rates in two areas of the Brazilian Amazon using LSMA.

STUDY AREAS

Two colonization areas were selected for this study (Figure 1). The Altamira study area is located along the Transamazon Highway in the Brazilian State of Para. The city of Altamira and the Xingu River anchor the eastern edge of the study area. In the 1950s colonists were attracted from northeast Brazil and settled along streams as far as 20 km from the city center. With the construction of the Transamazon Highway in 1970, this population and older caboclo settlers from the earlier rubber economic era claimed land along the new highway through the help of government-sponsored programs (Moran, 1976; 1981). Early settlement was driven by geopolitical goals and political economic policies that focused on occupying the region and establishing production areas of staples like rice, corn, and beans. This region has experienced a gradual shift to a more diverse set of land uses: pasture, cocoa, sugar cane, black pepper, in addition to staple crops. The dominant native vegetation types are mature moist forest and liana forest, but rates of deforestation and secondary succession associated with the implementation of agropastoral projects are high in the area.

The second study area is Machadinho in northeastern Rondônia. Rondônia had high deforestation rates in the Brazilian Amazon during the last twenty years (INPE, 2002). Following the national strategy of regional occupation and development, colonization projects initiated by the Brazilian government in the 1970s played a major role in this process (Moran, 1981; Schmink and Wood, 1992). Most colonization projects in Rondônia were designed to settle landless migrants. Settlement began in this area in the mid-1980s, and the immigrants transformed the forested landscape into a patchwork of cultivated crops, pastures, and a vast area of fallow land. The dominant pristine vegetation is tropical moist forest, with some bamboo and palms.

Figure 1. Locations of the Study Areas

METHOD

Image Preprocessing

Five dates of Thematic Mapper (TM) images and two scenes of IKONOS data in Altamira and three dates of TM images and one scene of IKONOS data in Machadinho were collected (Table 1). Of the various elements of

preprocessing for change detection, multi-date image registration and radiometric and atmospheric corrections are the most important. Accurate spatial registration of the multi-date imageries is obviously important for change detection because largely spurious results of change detection will be produced when misregistration between multi-date images occurs (Townshend et al., 1992; Dai and Khorram, 1998; Stow, 1999; Verbyla and Boles, 2000; Stow and Chen, 2002). The images were geometrically rectified into UTM projection using control points taken from topographic maps at 1:100,000 scale. The nearest-neighbor resampling technique was used and a root-mean squared error (RMSE) with less than 0.5 pixel was obtained. In Altamira, the 1991 TM image was first geometrically rectified, then other images were registered to it. In Machadinho, the 1998 TM image was first rectified, then other images were registered to the same projection as the 1998 TM image.

Table 1. Image Data and Field Data Used in Research

Study Areas	Altamira	Machadinho
Path/Row	226/62	231/67
TM acquisition dates	August 4, 1985 July 11, 1988 July 20, 1991 May 26, 1996 July 4, 2000 (ETM+)	Jul. 28, 1988 Jul. 15, 1994 Jun. 18, 1998
IKONOS data	October 14, 2000 (2 scenes)	May 28, 2001
Date to collect field data	1992, 1993, 1997, 1998	1999, 2000
Ancillary data	Topographic maps, DEM data, road vector layer	

Different image acquisition dates, sun elevation angles, and atmospheric conditions affect the remote sensing digital number (DN) values that are captured by satellite sensors. Accurately eliminating these impacts is necessary before the images are used for change detection analysis. A variety of methods have been developed for radiometric and atmospheric normalization or correction (Markham and Barker, 1987; Gilabert et al., 1994; Chavez, 1996; Stefan and Itten, 1997; Vermote et al., 1997; Heo and FitzHugh, 2000; Yang and Lo, 2000; Song et al., 2001; Lu et al., 2002; McGovern et al., 2002). Different models, such as relative normalization, dark object subtraction (DOS), and 6S, have their own characteristics and requirements for the input parameters. In this study, due to the lack of atmospheric data for the historical images, some advanced calibration models such as 6S were difficult to use. However, the image-based DOS model proved valuable for atmospheric correction when atmospheric data were not available (Lu et al., 2002). Hence, all TM data were calibrated into apparent reflectance using an image-based DOS model. The path radiance was identified based on clear water for each band.

Endmember Selection and Spectral Mixture Analysis

LSMA is regarded as a physically based image processing tool. It assumes that the spectrum measured by a sensor is a linear combination of the spectra of all components within the pixel (Adams et al., 1995; Roberts et al., 1998; Ustin et al., 1998; Petrou, 1999). It supports repeatable and accurate extraction of quantitative subpixel information (Smith et al., 1990; Roberts et al., 1998). The fractions derived from LSMA represent area proportions of the endmembers within the pixel. In remote-sensing data applications, the LSMA approach has been used for land-use/land-cover classification (Ustin et al., 1996; Cochrane and Souza, 1998; Ustin et al., 1999; Aguiar et al., 1999; DeFries et al., 2000; Theseira et al., 2002) and change detection (Adams et al., 1995; Roberts et al., 1997; Roberts et al., 1998; Shimabukuro et al., 1998; Ustin et al., 1998; Elmore et al., 2000; Rogan et al., 2002). In general, classification using LSMA involves four main steps: (1) image preprocessing, (2) endmember selection, (3) unmixing solution, and (4) analysis of fraction image.

Before using LSMA, it is necessary to reduce the high correlations that exist between visible TM bands. Standardized principal component analysis (SPCA) was used to transform the atmospherically calibrated TM imageries into principal components (PCs). The last two PCs were discarded due to their very limited information. Therefore, only the first four PCs were used for the LSMA approach to convert the images into physically based fractions.

Selecting suitable endmembers is the prerequisite to develop high quality fraction images. Different methods have been used for selecting endmembers (Adams et al., 1993; Settle and Drake, 1993; Boardman et al., 1995; Bateson and Curtiss, 1996; Tompkins et al., 1997; Mustard and Sunshine, 1999). For many remote-sensing applications using LSMA, the image-based endmember selection method is often used because endmembers can be

obtained easily, representing spectra measured at the same scale as the image data (Roberts et al., 1998). The endmembers are regarded as the extremes of the triangles of an image scattergram. Thus, the image endmembers are derived from the extremes of the image feature space, assuming they represent the purest pixels in the images (Mustard and Sunshine, 1999). In this study, three endmembers (shade, soil, and green vegetation or GV) were identified from the scattergram of the first two PCs derived from SPCA. An average of 30 to 50 pixels of these vertices was calculated. When selecting the endmembers, caution must be taken to identify outliers. Appropriate selection of image endmembers is often an iterative process. Checking fraction imageries and the RMSE image is a feasible way to assess whether the selected endmembers are appropriate or not (Lu et al., in press).

After selection of endmembers, an unconstrained least RMSE solution was used to unmix the first four PCs into three endmember fraction images. Detailed descriptions about LSMA and its applications can be found in Adams et al. (1995), Roberts et al. (1998), and Mustard and Sunshine (1999). Because the fractions represent the biophysical characteristics, different vegetation stand structures and land-cover types will have different proportion compositions. Hence, in this paper, the fraction images were used to identify mature forests and to analyze deforestation in the Brazilian Amazon through a change detection approach.

Change Detection and Accuracy Assessment

The use of LSMA to improve forest classifications is based on the fact that mature forest can be differentiated from other land-cover types through the analysis of fraction images. For example, mature forest has higher shade fraction but lower GV fraction than those of successional forests, pastures, and agricultural lands and has lower soil fraction than those of pasture, agricultural lands, and bare soil. From the soil fraction, mature forest and successional forest can be separated from pasture, agricultural land, bare soil, and urban areas. From the GV fraction, mature forest can be separated from successional forest, and from the shade fraction it can be separated from water bodies. Therefore, mature forest can be identified when the following conditions are satisfied:

$$(f_{soil} < T_{soil\_max}) \text{ and } (f_{GV} < T_{GV\_max}) \text{ and } (T_{shade\_min} < f_{shade} < T_{shade\_max}),$$

where f_{soil}, f_{GV}, and f_{shade} are fraction values of soil, GV, and shade, respectively. T_{soil_max}, T_{GV_max}, T_{shade_min}, and T_{shade_max} are thresholds of mature forest at each fraction image. The thresholds T_{soil_max}, T_{GV_max}, T_{shade_min}, and T_{shade_max} can be developed using sample plots of mature forest. A detailed description of threshold definition based on field data and fraction images can be found in Lu et al. (in press). A total of 25 sample plots of mature forest were identified, and descriptive statistics were produced. The statistical parameters include minimum, maximum, mean, and standard deviation. So, the threshold of mature forest in each fraction is defined as:

$$T_{soil\_max} = T_{soil\_u} + \gamma * \sigma_{soil},$$

$$T_{GV\_max} = T_{GV\_u} + \gamma * \sigma_{GV},$$

$$T_{shade\_min} = T_{shade\_u} - \gamma * \sigma_{shade}, \text{ and}$$

$$T_{shade\_max} = T_{shade\_u} + \gamma * \sigma_{shade},$$

where T_{soil_u}, T_{GV_u}, and T_{shade_u} are mean values and σ_{soil}, σ_{GV}, and σ_{shade} are standard deviations, which are derived from the sample plots of soil, GV, and shade fraction images, respectively. γ is a constant. Different constants were tested, ranging from 2.5 to 3.5, in order to find a best constant for the identification of mature forest.

After selection of appropriate thresholds for each fraction image, the thresholds were then used for the entire study area to produce a binary image, indicating mature forest and non-forest (1 as mature forest and 0 as non-forest). The same procedure was implemented for all TM images in both study areas listed in Table 1, beginning from SPCA, endmember selection, development of fractions, and until identification of mature forest. After finishing classification of mature forest and non-forest for all TM images, the binary thematic images were added to produce a new thematic image for each study area for change detection. For example, in the Machadinho study area, TM images from 1988, 1994, and 1998 were used, and three corresponding binary images were produced using LSMA and thresholds. Adding the three binary images produces a thematic image with pixel values ranging from 0 to 3. Thus, the following change information can be inferred:

0 – unchanged non-forest areas,

1 – deforestation, converting mature forest in 1988 to non-forest in 1994,

2 – deforestation, converting mature forest in 1994 to non-forest in 1998,

3 – unchanged mature forest.

To test the validity of the procedure, accuracy assessment is an important part in both classification and change detection routines. A common method for accuracy assessment is through the use of an error matrix. Previous literature has provided the meanings and calculation methods for overall accuracy, producer's accuracy, user's accuracy, and kappa coefficient (Congalton et al., 1983; Hudson and Ramm, 1987; Congalton, 1991; Janssen and van der Wel, 1994; Kalkhan et al., 1997; Khorram, 1999; Smits et al., 1999). In this paper, overall accuracy was calculated for each classification and change detection result. A total of 240 sample plots were randomly allocated and examined through visual interpretation assisted by field data and IKONOS data for analyses of classification and change detection accuracies.

RESULTS AND DISCUSSION

The LSMA approach was used to develop fraction images for all dates of TM images for both study areas, respectively. Figure 2 provides an example of fraction images in Altamira (2000 ETM+ image) and Machadinho (1998 TM image). Mature forest in the soil fraction image appears dark grey due to its very low soil fraction. It appears grey in the GV fraction and bright grey in the shade fraction. Thus, mature forest has different characteristics in each fraction image and can be distinguished from non-forest vegetation based on these fraction images.

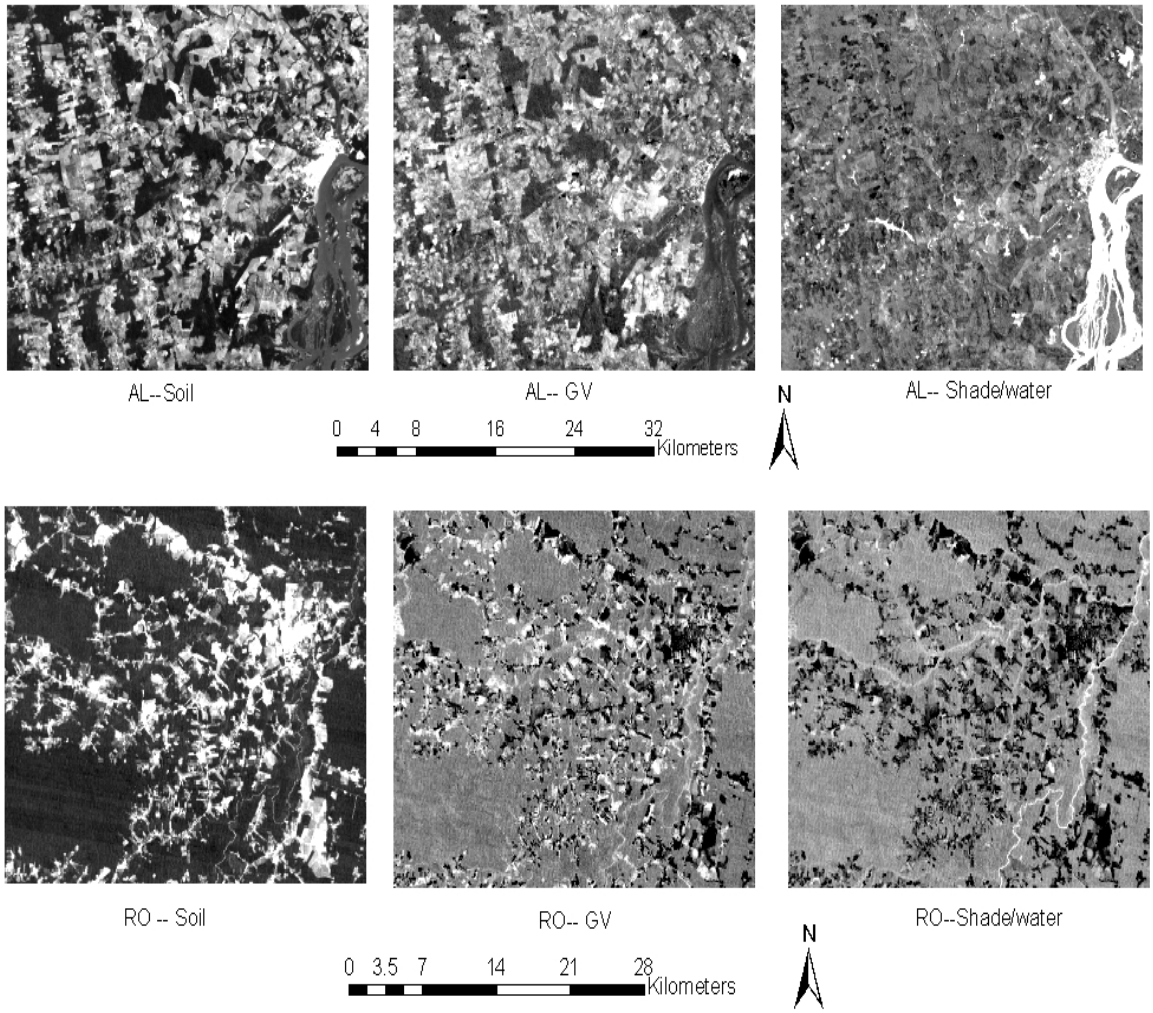

Figure 2. Fraction Images in Altamira (AL, 2000 ETM+) and Machadinho, Rondônia (RO, 1998 TM)

Figure 3 gives a comparison of fraction values of main land-cover types and illustrates the physical features of different land-cover types in these fraction images. It indicates that mature forest and secondary successional forests have significantly lower soil fractions than those of pasture, agricultural lands, and bare lands. Mature forest has lower fractions in the GV fraction image but has higher fractions in the shade fraction image than those of successional forests, pastures, and agricultural lands. This characteristic of mature forest in different fraction images enables us to accurately distinguish non-forest types and yields better results when thresholds are appropriately selected on each fraction image.

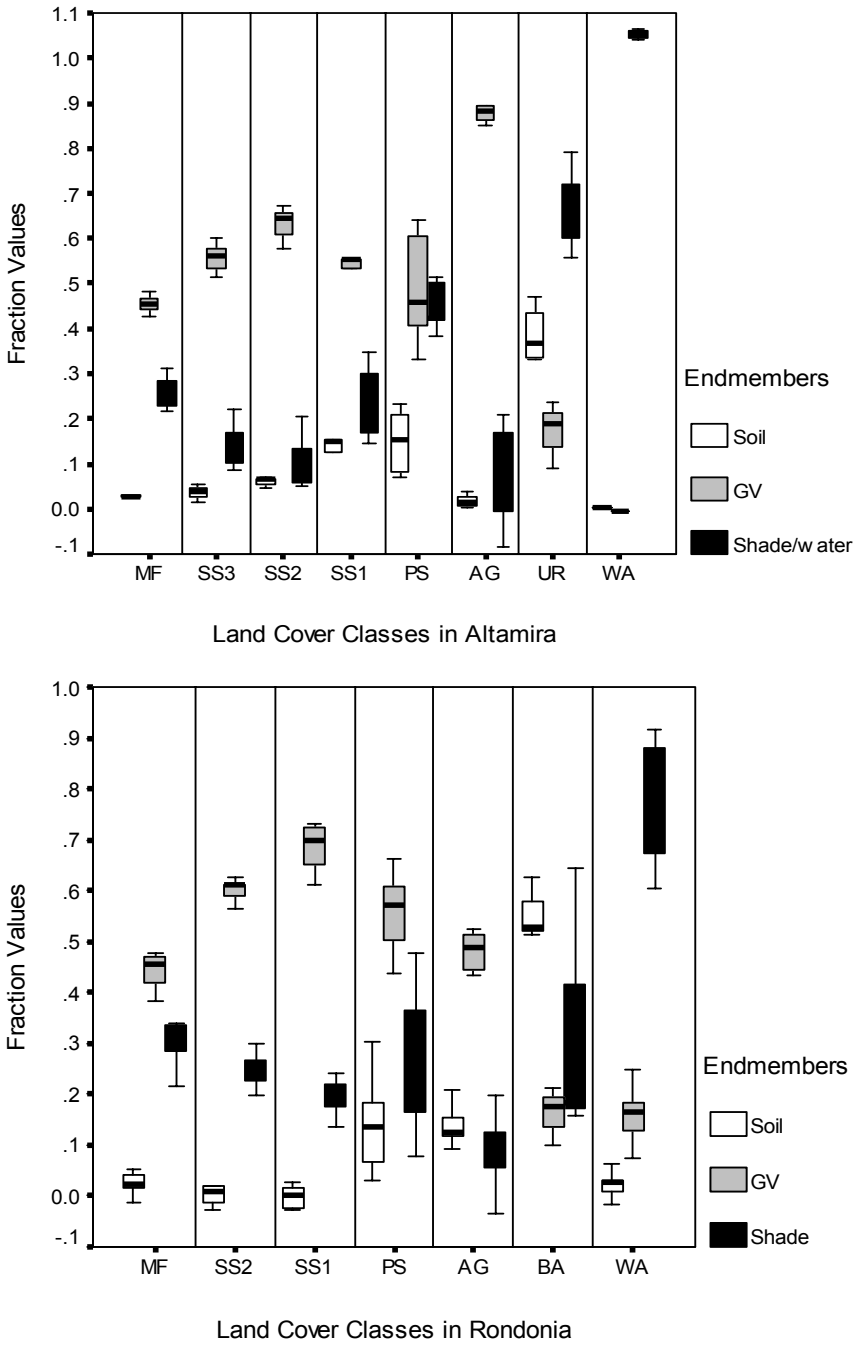

Figure 3. Comparison of Fractions among Typical Land-cover Classes in Altamira (AL, 2000 ETM+) and Machadinho, Rondônia (RO, 1998 TM)

Figure 4 illustrates the deforestation area distribution using five dates of TM images in Altamira and three dates of TM images in Machadinho. A road vector layer was overlaid on the change detection image to show the spatial relationship between deforestation and road configuration. The deforestation process is closely related to the road construction. For example, mature forest was often deforested along both sides of the roads, then extended to wide areas. Most deforestation in the Altamira study area occurred in the 1970s and early 1980s, and very limited mature forest remained until 2000. In the Machadinho study area, most of the terrain was still occupied by mature forest because of the presence of large patches of forest preserved in extractive reserves (Batistella, 2001). However, deforestation is obvious along the sides of the roads.

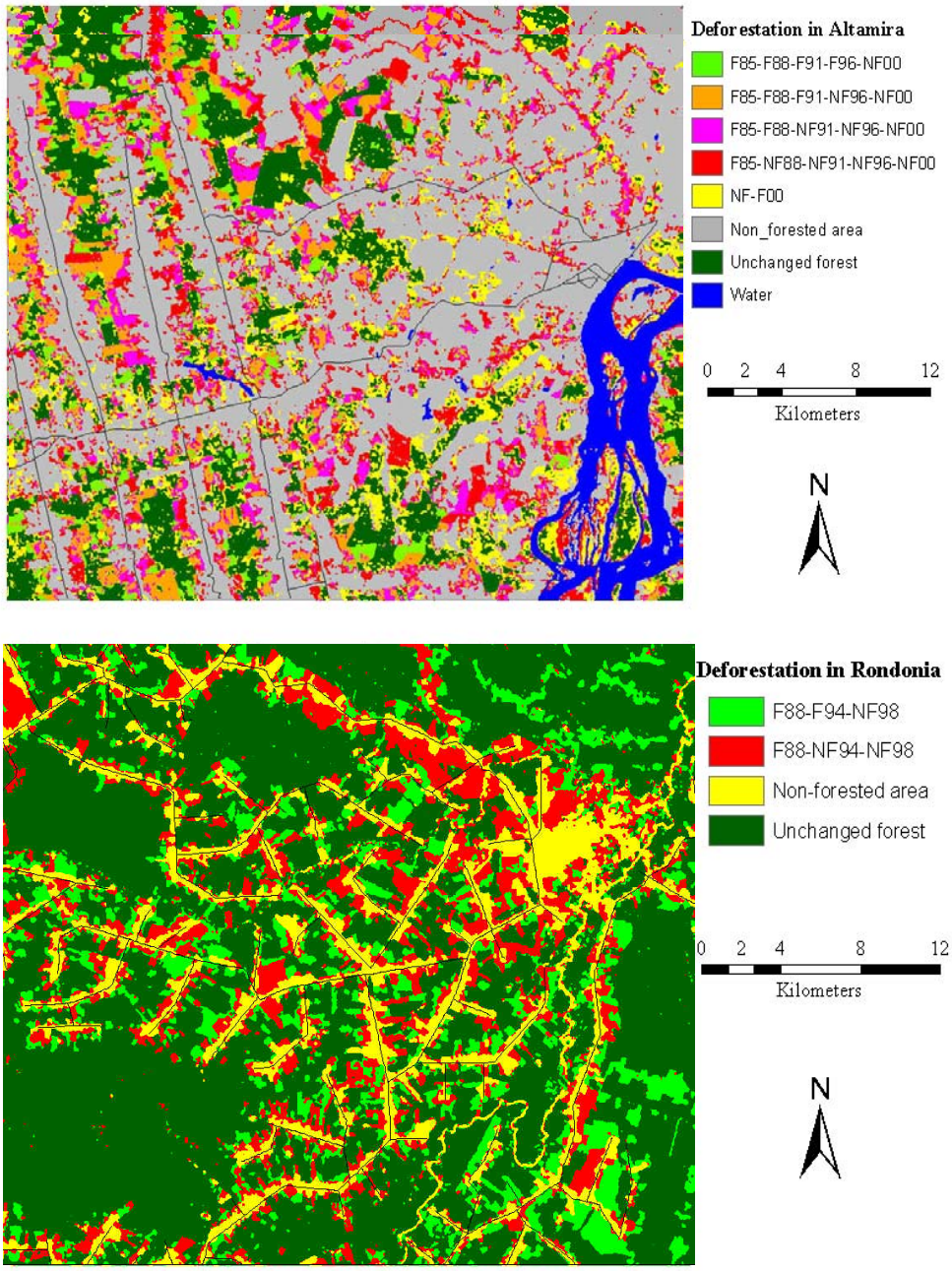

Figure 4. Deforestation Area Distribution in Altamira and Machadinho

The deforested area and deforestation rate were calculated for each change detection period for both study areas. Table 2 provides the results in selected detection periods in Altamira and Machadinho. In Altamira, the deforestation rate is decreasing because the remaining mature forest area is very limited and most of the mature forest already has been cut. In Machadinho, the deforestation rate is increasing because colonization began in the middle 1980s. However, mature forest still occupies the majority of the study area. In Altamira, the deforested mature forest accounts for 26.18% of the total study area during the 15-year period between 1985 and 2000. Higher deforestation rates occurred during the 1970s and early 1980s. In the Machadinho study area, the deforested mature forest accounts for 27.32% of the total study area during the 10-year period between 1988 and 1998.

Table 2. Mature Forest Change Detection Results

Altamira Study Area								
	Mature Forest Deforestation				Others			Total Area
	1985-88	1988-91	1991-96	1996-00	NF_unchg	F_unchg	NF_to_F	
Def. area (ha)	11054.70	6517.89	7598.16	3652.56	56569.77	14415.48	10249.92	110058.48
Def. rate (%)	10.04	5.92	6.90	3.32				
Avg. def rate	3.35	1.97	1.38	0.83				

Machadinho, Rondônia, Study Area					
	Mature Forest Deforestation		Others		Total Area
	1988-94	1994-98	NF_unchg	F_unchg	
Def. area (ha)	14389.38	12767.76	14350.14	57896.64	99403.92
Def. rate (%)	14.48	12.84			
Avg Def. rate	2.41	3.21			

Note: Def. Rate (%) = deforestation area/total study area *100.
Avg Def. rate (%/yr) = def. rate/change-detection-period.
NF_unchg: unchanged non-forest.
F_unchg: unchanged forest.
NF_to_F: non-forest in previous date change to forest in late date.

Many test sample data were collected and used for classification and change detection accuracy assessment. An error matrix for each classification and change detection result was produced and overall accuracy was provided. Table 3 provides the overall classification and change detection accuracies in Altamira and Machadinho. The classification accuracy of mature forest is very high, reaching over 98.7%, and the change detection accuracy reaches over 96% in both study areas. These results indicated that deforestation detection using LSMA is reliable and successful.

Table 3. Classification and Change Detection Accuracies

Study Area	Classification Accuracy			Change Detection Accuracy	
Altamira	1991	1996	2000	1991–1996	1996–2000
	98.7%	99.3%	99.3%	98.0%	96.0%
Machadinho	1994	1998		1994-1998	
	98.7%	98.7%		96.7%	

Analysis of the classification and change detection results found that the errors were mainly from (1) clouds and cast shadows, especially thin clouds and cast shadows; and (2) complex landscape and environmental conditions, such as mature forests in wetland sites. The thin clouds and their cast shadows and the significantly different moisture conditions in the sites of mature forest affect the fraction values developed using LSMA. One possible solution is to stratify the entire image into some subset images with similar environmental conditions within the

subset image. Then selecting endmembers and unmixing TM images could be carried out in the subset images respectively. Caution needs to be taken to separate the true reflectance of endmembers and outliers, for example, clouds.

After development of fraction images using LSMA, the classification and change detection accuracies are greatly dependent on the definition of thresholds. In this paper, different standard deviations were tested and the results were analyzed. This experiment indicated that three standard deviations provided the best threshold ranges for the mature forest classification.

CONCLUSION

The LSMA approach has been successfully used in this paper for mature forest classification and deforestation detection. The classification accuracies of mature forest reached over 98.7% and the change detection accuracies reached over 96% for TM images of different dates for both study areas in the Brazilian Amazon. When using LSMA, selection of appropriate endmembers is very important to develop high-quality fraction images. SPCA is an effective transformation method in reducing correlation coefficients between images used, thus, improving the fraction images. Definition of thresholds for mature forest is critical to produce highly accurate classification and change detection results.

ACKNOWLEDGMENTS

The authors wish to thank the National Science Foundation (grants SBR-95-21918 and 99-06826), the National Aeronautics and Space Administration (grant N005-334), and Brazil's Program for the Advancement of Education for their support, which provided funds for the research that led to this paper. This project is part of the Large-Scale Biosphere-Atmosphere (LBA) Experiment in Amazônia program, LC-09, which examines the human and physical dimensions of land-use and land-cover change. We also thank Indiana State University and Indiana University for facilities and support of our work; our collaborators in Brazil, especially the LBA Program, Empresa Brasileira de Pesquisa Agropecuária (Embrapa), Instituto Nacional de Pesquisas Espaciais (INPE); and the population of the study area, who made this work possible.

REFERENCES

Adams, J. B., Smith, M. O., and Gillespie, A. R. (1993). Imaging spectroscopy: interpretation based on spectral mixture analysis. In: C. M. Pieters and P. A. J. Englert (Editors). *Remote Geochemical Analysis, Topics in Remote Sensing 4*. Cambridge University Press, Cambridge, U.K., pp. 145–166.

Adams, J. B., Sabol, D. E., Kapos, V., Filho, R. A., Roberts, D. A., Smith, M. O., and Gillespie, A. R. (1995). Classification of multispectral images based on fractions of endmembers: application to land-cover change in the Brazilian Amazon. *Remote Sensing of Environment,* **52**: 137–154.

Aguiar, A. P. D., Shimabukuro, Y. E., and Mascarenhas, N. D. A. (1999). Use of synthetic bands derived from mixing models in the multispectral classification of remote sensing images. *International Journal of Remote Sensing,* **20**: 647-657.

Alves, D. S. (2002). Space-time dynamics of deforestation in Brazilian Amazonia. *International Journal of Remote Sensing,* **23**: 2903-2908.

Bateson, A., and Curtiss, B. (1996). A method for manual endmember selection and spectral unmixing. *Remote Sensing of Environment,* **55**: 229–243.

Batistella, M. (2001). *Landscape Change and Land-Use/Land-Cover Dynamics in Rondônia, Brazilian Amazon*. Ph.D. diss. University Graduate School and the School of Public and Environmental Affairs, Indiana University, USA. CIPEC Dissertation Series, No. 7. Bloomington: Center for the Study of Institutions, Population, and Environmental Change, Indiana University.

Boardman, J. M., Kruse, F. A., and Green, R. O. (1995). Mapping target signature via partial unmixing of AVIRIS data. In: *Summaries of the Fifth JPL Airborne Earth Science Workshop,* JPL Publication 95-1, pp. 23–26.

Chavez, P. S. Jr. (1996). Image-based atmospheric corrections – revisited and improved. *Photogrammetric Engineering and Remote Sensing*, **62**: 1025–1036.

Cochrane, M. A., and Souza, C. M. Jr. (1998). Linear mixture model classification of burned forests in the eastern Amazon. *International Journal of Remote Sensing,* **19:** 3433-3440.

Congalton, R. G., Oderwald, R. G., and Mead, R. A. (1983). Assessing Landsat classification accuracy using discrete multivariate analysis statistical techniques. *Photogrammetric Engineering and Remote Sensing,* **49:** 1671-1678.

Congalton, R. G. (1991). A review of assessing the accuracy of classification of remotely sensed data. *Remote Sensing of Environment,* **37**: 35–46.

Coppin, P.R., and Bauer, M. E. (1996), Digital change detection in forest ecosystems with remote sensing imagery. *Remote Sensing Reviews,* **13**: 207–234.

Dai, X. L., and Khorram, S. (1998). The effects of image misregistration on the accuracy of remotely sensed change detection. *IEEE Transactions on Geoscience and Remote Sensing,* **36**: 1566-1577.

Deer, P.J. (1995). Digital change detection techniques: civilian and military applications. In: *International Symposium on Spectral Sensing Research '95 Report*, November 26–December 1, Melbourne, Australia.

DeFries, R. S., Hansen, M. C., and Townshend, J. R. G. (2000). Global continuous fields of vegetation characteristics: a linear mixture model applied to multi-year 8km AVHRR data. *International Journal of Remote Sensing,* **21**: 1389-1414.

Elmore, A. J., Mustard, J. F., Manning, S. J., and Lobell, D. B. (2000). Quantifying vegetation change in semiarid environments: precision and accuracy of spectral mixture analysis and the normalized difference vegetation index. *Remote Sensing of Environment,* **73**: 87-102.

Fearnside, P.M. (1998). Forests and global warming mitigation in Brazil: opportunities in the Brazilian forest sector for responses to global warming under the "clean development mechanism." *Biomass and Bioenergy,* **00**: 1–19.

Gilabert, M. A., Conese, C., and Maselli, F. (1994). An atmospheric correction method for the automatic retrieval of surface reflectance from TM images. *International Journal of Remote Sensing,* **15**: 2065-2086.

Heo, J., and FitzHugh, T. W. (2000). A standardized radiometric normalization method for change detection using remotely sensed imagery. *Photogrammetric Engineering and Remote Sensing,* **66**: 173-182.

Houghton, R.A. (1991). Tropical deforestation and atmospheric carbon dioxide. *Climatic Change,* **19**: 99–118.

Hudson, W. D., and Ramm, C. W. (1987). Correct formulation of the Kappa coefficient of agreement. *Photogrammetric Engineering and Remote Sensing,* **53**: 421-422.

Instituto Nacional de Pesquisas Espaciais (INPE) (1998). *Amazonia: Deforestation 1995–1997*. INPE, Sao Jose dos Campos, Sao Paulo-Brazil.

———. (2002). *Monitoring of the Brazilian Amazon forest by satellite 2000-2001*, INPE, Brazil.

Janssen, L. F. J., and van der Wel, F. J. M. (1994). Accuracy assessment of satellite derived land-cover data: a review. *Photogrammetric Engineering and Remote Sensing,* **60:** 419–426.

Jensen, J.R. (1996). *Introductory Digital Image Processing: A Remote Sensing Perspective*, 2d ed., Prentice Hall, Upper Saddle River, NJ-USA.

Jensen, J. R., Cowen, D., Narumalani, S., and Halls, J. (1997). Principles of change detection using digital remote sensor data. In: *Integration of Geographic Information Systems and Remote Sensing.* J. L. Star, J. E. Estes, and K. C. McGwire (Editors). Cambridge: Cambridge University Press, pp. 37-54.

Kalkhan, M. A., Reich, R. M., and Czaplewski, R. L. (1997). Variance estimates and confidence intervals for the Kappa measure of classification accuracy. *Canadian Journal of Remote Sensing,* **23:** 210–216.

Khorram, S. (ed.) (1999) *Accuracy assessment of remote sensing–derived change detection*. Monograph Series, American Society for Photogrammetry and Remote Sensing, Bethesda, Md.

Lu, D., Mausel, P., Brondizio, E., and Moran, E. (2002). Assessment of atmospheric correction methods for Landsat TM data applicable to Amazon basin LBA research. *International Journal of Remote Sensing,* **23:** 2651-2671.

Lu, D., Moran, E., and Batistella, M. (in press) Linear mixture model applied to Amazônian vegetation classification. *Remote Sensing of Environment*.

Markham, B. L., and Barker, J. L. (1987). Thematic Mapper bandpass solar exoatmospheric irradiances. *International Journal of Remote Sensing,* **8**: 517-523.

McGovern, E. A., Holden, N. M., Ward, S. M., and Collins, J. F. (2002). The radiometric normalization of multitemporal Thematic Mapper imagery of the midlands of Ireland – a case study. *International Journal of Remote Sensing*, **23**: 751-766.

Moran, E. F. (1976). *Agricultural development along the Transamazôn highway*. Center for Latin American Studies Monograph, Indiana University, Bloomington, pp 136.

———. (1981). *Developing the Amazon*. Indiana University Press, Bloomington, Ind.

Moran. E.., Brondizio, E., Mausel, P., and Wu, Y. (1994). Integrating Amazonian vegetation, land use, and satellite data. *Bioscience,* **44:** 329–338.

Mouat, D.A., Mahin, G. C., and Lancaster, J. (1993). Remote sensing techniques in the analysis of change detection. *Geocarto International,* **8:** 39–50.

Mustard, J. F., and Sunshine, J. M. (1999). Spectral analysis for earth science: investigations using remote sensing data. In: A. N. Rencz (Editor), *Remote Sensing for the Earth Sciences: Manual of Remote Sensing*, 3d edition, vol. 3. John Wiley and Sons, Inc., New York, pp. 251–307.

Petrou, M. (1999). Mixed pixel classification: an overview. In: C. H. Chen (Editor), Information Processing for Remote Sensing, World Scientific Publishing Co., Singapore, pp. 69-83.

Roberts, D. A., Batista, G. T., Pereira, J. L. G., Waller, E. K., and Nelson, B. W. (1998). Change identification using multitemporal spectral mixture analysis: applications in eastern Amazônia. In: R. S. Lunetta and C. D. Elvidge (Editors), *Remote Sensing Change Detection: Environmental Monitoring Methods and Applications*. Ann Arbor Press, Ann Arbor, Mich., pp. 137–161.

Roberts, D. A., Green, R. O., and Adams, J. B. (1997). Temporal and spatial patterns in vegetation and atmospheric properties from AVIRIS. *Remote Sensing of Environment,* **62**: 223-240.

Rogan, J., Franklin, J., and Roberts, D. A. (2002). A comparison of methods for monitoring multitemporal vegetation change using Thematic Mapper imagery. *Remote Sensing of Environment,* **80**: 143-156.

Schmink, M., and Wood, C. H. (1992). *Contested Frontiers in Amazônia*. Columbia University Press, New York.

Serpico, S. B., and Bruzzone, L. (1999). Change detection. In *Information Processing for Remote Sensing*, edited by C. H. Chen, Singapore: World Scientific Publishing Co. Pte. Ltd, pp.319-336.

Settle, J. J., and Drake, N. A. (1993). Linear mixing and the estimation of ground cover proportions. *International Journal of Remote Sensing,* **14**: 1159–1177.

Shimabukuro, Y. E., Batista, G. T., Melio, E. M. K., Moreira, J. C. and Duarte, V. (1998). Using shade fraction image segmentation to evaluate deforestation in Landsat Thematic Mapper images of the Amazon region. *International Journal of Remote Sensing,* **19**: 535-541.

Shukla, J., Nobre, C., and Sellers, P. (1990). Amazôn deforestation and climate change. *Science,* **247:** 1322–1325.

Singh, A. (1989). Digital change detection techniques using remotely sensing data. *International Journal of Remote Sensing,* **10**: 989–1003.

Skole, D., Chomentowski, W.H., Salas, W.A., and Nobre, A. D. (1994). Physical and human dimensions of deforestation in Amazônia. *Bioscience,* **44:** 314–322.

Skole, D. L., and Tucker, C. (1993). Tropical deforestation and habitat fragmentation in the Amazon: satellite data from 1978 to 1988. *Science,* **260:** 1905–1909.

Smith, M. O., Ustin, S. L., Adams, J. B., and Gillespie, A. R. (1990). Vegetation in Diserts: I. A regional measure of abundance from multispectral images. *Remote Sensing of Environment,* **31**: 1-26.

Smits, P. C., Dellepiane, S. G., and Schowengerdt, R. A. (1999). Quality assessment of image classification algorithms for land-cover mapping: a review and a proposal for a cost-based approach. *International Journal of Remote Sensing,* **20**: 1461–1486.

Song, C., Woodcock, C.E., Seto, K. C., Lenney, M.P., and Macomber, S.A. (2001). Classification and change detection using Landsat TM data: when and how to correct atmospheric effect. *Remote Sensing of Environment,* **75**: 230-244.

Stefan, S., and Itten, K. I. (1997). A physically-based model to correct atmospheric and illumination effects in optical satellite data of rugged terrain. *IEEE Transactions on Geoscience and Remote Sensing*, **35**: 708-717.

Stow, D. A. (1999). Reducing the effects of misregistration on pixel-level change detection. *International Journal of Remote Sensing*, **20**: 2477-2483.

Stow, D. A., and Chen, D.M. (2002). Sensitivity of multitemporal NOAA AVHRR data of an urbanizing region to land-use/land-cover change and misregistration. *Remote Sensing of Environment*, **80**: 297-307.

Theseira, M. A., Thomas, G., and Sannier, C. A. D. (2002). An evaluation of spectral mixture modeling applied to a semi-arid environment. *International Journal of Remote Sensing,* **23**: 687-700.

Tompkins, S., Mustard, J. F., Pieters, C. M., and Forsyth, D. W. (1997). Optimization of endmembers for spectral mixture analysis. *Remote Sensing of Environment,* **59**: 472-489.

Townshend, J. R. G., Justice, C. O., Gurney, C., and McManus, J. (1992). The effect of image misregistration on the detection of vegetation change. *IEEE Transactions on Geoscience and Remote Sensing*, **30**: 1054-1060.

Ustin, S. L., Hart, Q. J., Duan, L., and Scheer, G. (1996). Vegetation mapping on hardwood rangelands in California. *International Journal of Remote Sensing,* **17**: 3015-3036.

Ustin, S. L., Roberts, D. A., and Hart, Q. J. (1998) Seasonal vegetation patterns in a California coastal savanna derived from Advanced Visible/Infrared Imaging Spectrometer (AVIRIS) data. In: R. S. Lunetta and C.D.

Elvidge (Editors), *Remote Sensing Change Detection: Environmental Monitoring Methods and Applications*. Ann Arbor Press, Ann Arbor, Mich., pp. 163–180.

Ustin, S. L., Smith, M. O., Jacquemoud, S., Verstraete, M., and Govaerts, Y. (1999). Geobotany: vegetation mapping for Earth sciences. In: A. N. Rencz (Editor), Remote Sensing for the Earth Sciences: Manual of Remote Sensing, 3rd edition, Vol. 3, John Wiley & Sons, Inc., pp. 189-233.

Verbyla, D. L., and Boles, S. H. (2000). Bias in land cover change estimates due to misregistration. *International Journal of Remote Sensing,* **21**: 3553-3560.

Vermote, E., Tanre, D., Deuze, J. L., Herman, M., and Morcrette, J. J. (1997). Second simulation of the satellite signal in the solar spectrum, 6S: An overview. *IEEE Transactions on Geoscience and Remote Sensing,* **35:** 675-686.

Yang, X., and Lo, C. P. (2000). Relative radiometric normalization performance for change detection from multi-date satellite images. *Photogrammetric Engineering and Remote Sensing,* **66**: 967-980.

Yuan, D., Elvidge, C. D., and Lunetta, R. S. (1998). Survey of multispectral methods for land cover change analysis. In *Remote Sensing Change Detection: Environmental Monitoring Methods and Applications*, edited by R. S. Lunetta and C. D. Elvidge, Ann Arbor Press (Chelsea, MI), pp. 21-39.